

Figure S1

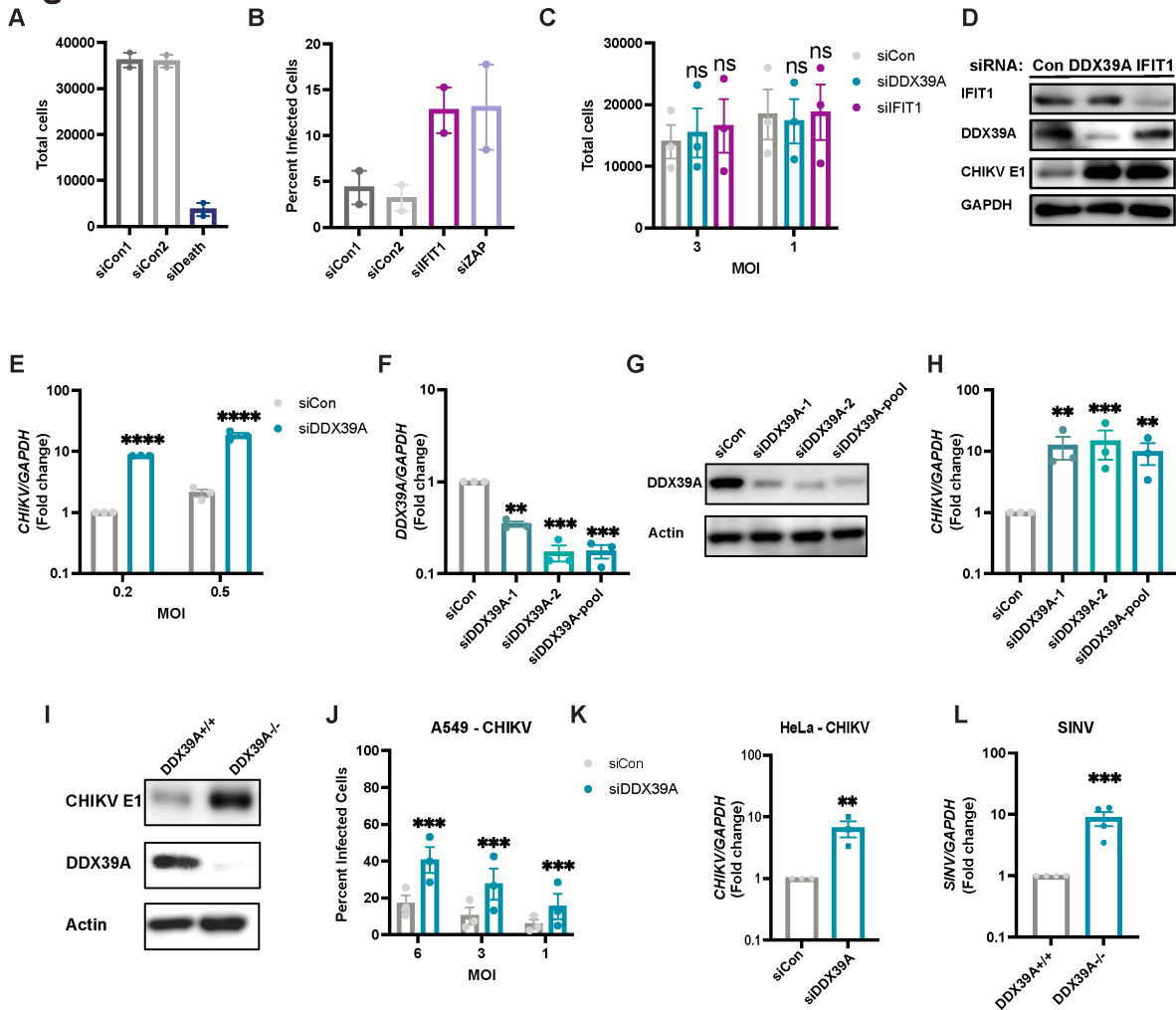


Figure S1. DDX39A is antiviral against CHIKV, Related to Figure 1.

(A-B) U2OS cells were transfected with scrambled siRNAs as negative controls (siCon1 and siCon2) and siRNAs against IFIT1 and ZAP as positive controls. siRNAs targeting anti-apoptotic genes (siDeath) were used for RNAi efficiency. Cells were infected (CHIKV Ross MOI 0.1, 24h), stained (nuclei, Hoechst 33342 and infection, anti-CHIKV), and imaged and analyzed with automated microscopy, n=2. (C) Control, DDX39A, and IFIT1-depleted cells were infected with CHIKV at the indicated MOIs. Cell viability was quantified (nuclei+) relative to negative siRNA controls using automated microscopy. (D) Transfected cells were infected with CHIKV (MOI 0.5), and lysates were probed for DDX39A and IFIT1 to confirm gene knockdown and for CHIKV E1 to assess infection. GAPDH was used as a loading control. n=2, representative image shown. (E) Control and DDX39A-depleted cells were infected with CHIKV at the indicated MOIs, and viral RNA was quantified by qPCR. (F-H) DDX39A was depleted using either two independent or pooled siRNAs followed by infection with CHIKV (MOI 0.5, 24h). (F) *DDX39A* mRNA and (G) viral RNA levels were measured by qPCR and (H) DDX39A protein levels were determined by immunoblot. (I) DDX39A^{-/-} U2OS cells were generated using CRISPR/Cas9 and infected with CHIKV (MOI 0.1, 24h). DDX39A and CHIKV E1 viral protein levels were assessed by immunoblot. (J) Control and DDX39A-depleted A549 cells were infected with CHIKV at the indicated MOIs for

24h and infection was assessed by automated microscopy. (K) Control and DDX39A-depleted HeLa cells were infected with CHIKV (MOI 0.5, 24h), and viral RNA was quantified by qPCR. (L) *DDX39A*^{-/-} U2OS were infected with SINV mKate (MOI 0.1, 24h), and SINV RNA was measured by qPCR. Data are presented as fold change vs. control cells in (E, F, H, K, L). Dots represent individual knockdown experiments, n=3 for all experiments unless otherwise indicated. *GAPDH* was used as a loading control gene for all qPCR experiments unless otherwise noted. Beta-Acting was used as a loading control for all immunoblots as indicated. Statistical analyses were performed using two-way ANOVA with Bonferroni corrections for multiple comparisons (C, E, J), one-way ANOVA with Bonferroni corrections for multiple comparisons (F, H), and Student's (unpaired, two-tailed) *t*-test (K, L). *p<0.05, **p<0.01, ***p<0.001, ****p<0.0001; error bars represent S.E.M.

Figure S2

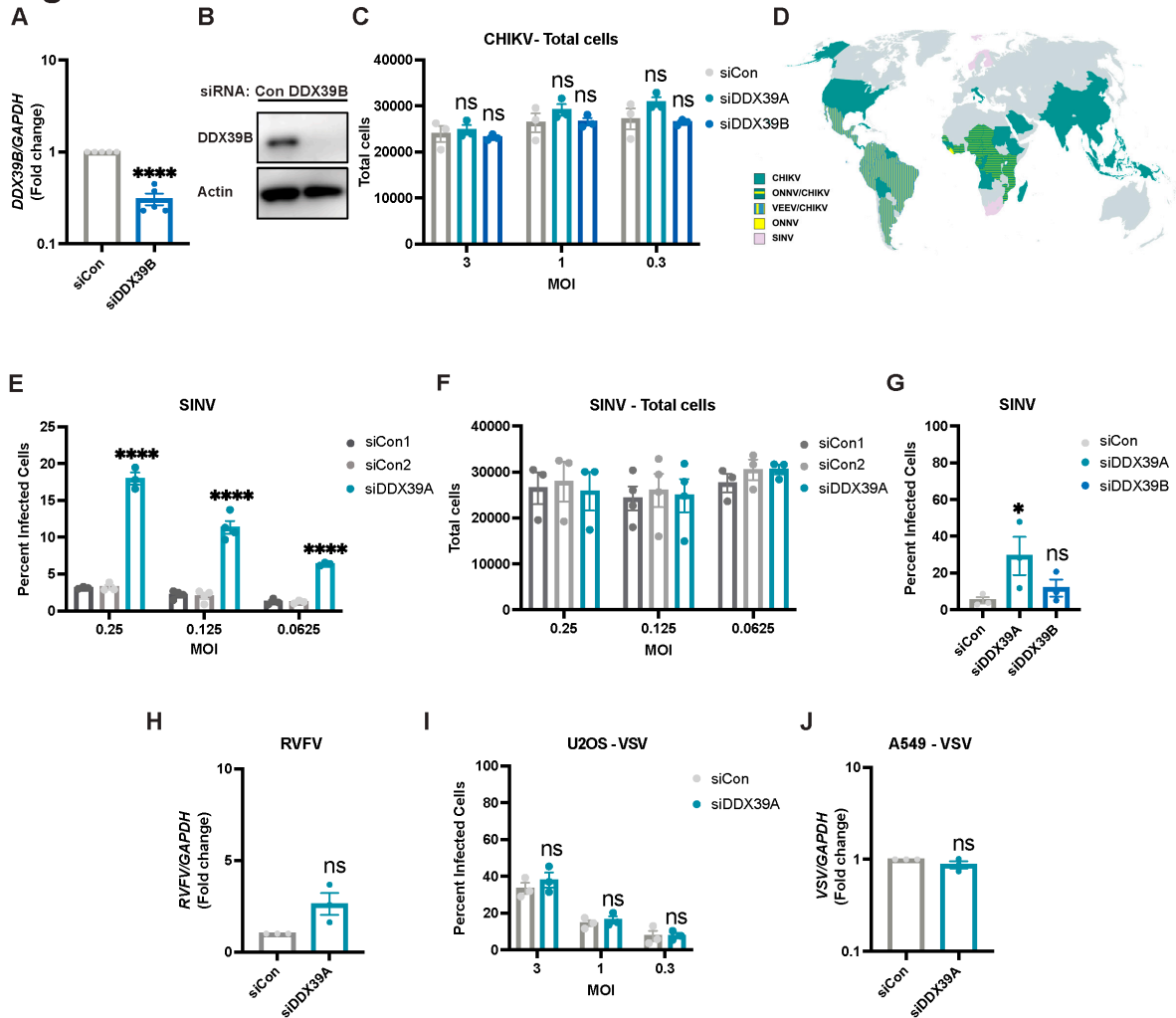


Figure S2. DDX39A, but not DDX39B, is antiviral against alphaviruses, Related to Figure 1.

(A-B) Knockdown of DDX39B in U2OS cells was assessed by (A) qPCR and by (B) immunoblot. (C) Control, DDX39A, and DDX39B-depleted U2OS cells infected with CHIKV at the indicated MOIs for 24h. Cell number was measured using Hoechst 33342 for nuclei and automated microscopy. (D) Global distribution of the alphaviruses used in this study. Generated with mapchart.net based on current literature¹⁻⁴. (E-F) Control and DDX39A-depleted U2OS cells were infected with SINV-mKate at the indicated MOIs for 24h. Cells were stained (nuclei, Hoechst 33342), and imaged. (E) Percent infected cells and (F) total cells were calculated with automated microscopy. (G) DDX39A and DD39B-depleted U2OS cells were infected with SINV-mKate (MOI 0.5, 24h) and the percent infected cells were quantified by automated microscopy. (H-I) U2OS cells depleted of DDX39A were infected with (H) Rift Valley fever virus (RVFV, MOI 0.1, 24h) or (I) VSV-GFP at the indicated MOIs for 16h, and infection was assessed by (H) qPCR for viral RNA or by (I) immunofluorescence with automated microscopy. (J) A549 depleted of control or DDX39A were infected with VSV, and infection was assessed by qPCR. Dots represent individual knockdown experiments, n=3-5 for all experiments. Data are presented as fold change vs. control cells in (A, H, J). *GAPDH* was used as a loading control gene for all qPCR experiments unless

otherwise noted. Beta-Actin was used as a loading control for immunoblots. Statistical analyses were performed using two-way ANOVA with Bonferroni corrections for multiple comparisons (C, E, I), one-way ANOVA with Bonferroni corrections for multiple comparisons (G), and Student's (unpaired, two-tailed) *t*-test (A, H, J). * $p < 0.05$, ** $p < 0.01$, *** $p < 0.001$, **** $p < 0.0001$; error bars represent S.E.M.

Figure S3

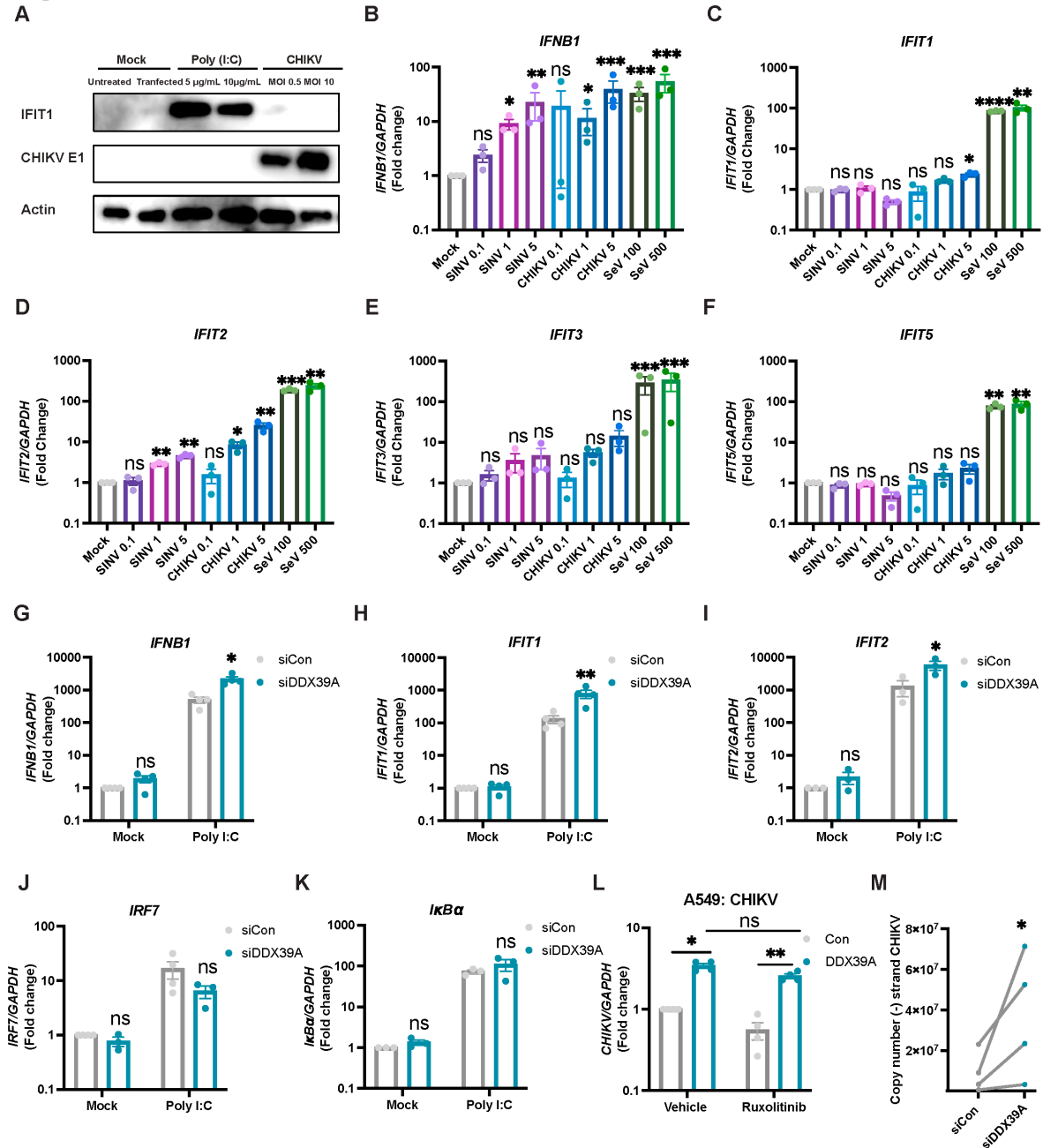


Figure S3. DDX39A is not required for the induction of the IFN pathway, Related to Figures 2 and 3.

(A) U2OS cells were mock transfected, stimulated with poly (I:C) at the indicated concentrations, and infected with CHIKV at the indicated MOIs. Viral and innate immune protein expression was assessed by immunoblot. Representative image shown. (B-F) U2OS cells were infected with SINV-mKate (MOIs 0.1,1,5), CHIKV (MOIs 0.1,1,3) or SeV (100 and 500 HAU/mL), and levels of *IFNB1* or the indicated ISGs were assessed by qPCR compared to mock uninfected cells. (G-L) U2OS cells depleted of control and DDX39A were transfected with either vehicle or poly (I:C) for 6-8h. Levels of (G) *IFNB1*, (H) *IFIT1*, (I) *IFIT2*, (J) *IRF7*, and (J) *Ikbα* transcript levels were

measured by qPCR. (L) Control or siRNA depleted-DDX39A A549 cells were pretreated with vehicle or Ruxolitinib (10 μ M) and infected with CHIKV (MOI 1, 24h). Levels of viral RNA were measured by qPCR. (M) (-) strand (antigenome) copy numbers were quantified using strand-specific RT-qPCR in control and DDX39A-depleted U2OS cells infected with CHIKV (MOI 20, 4h). *GAPDH* was used as a loading control gene for qPCRs in (B-K). Data are shown as fold change relative to mock siCon. Dots represent individual experiments, n=3-4 for all experiments. Beta-Actin was used as a loading control for immunoblots. Statistical analyses were performed using one-way ANOVA with Dunnett's correction for multiple comparisons (B-F), two-way ANOVA with Bonferroni corrections for multiple comparisons (G-K), paired t-test (M), and two-way ANOVA with Turkey's correction for multiple comparisons (L). *p<0.05, **p<0.01, ***p<0.001, ****p<0.0001; error bars represent S.E.M.

Figure S4

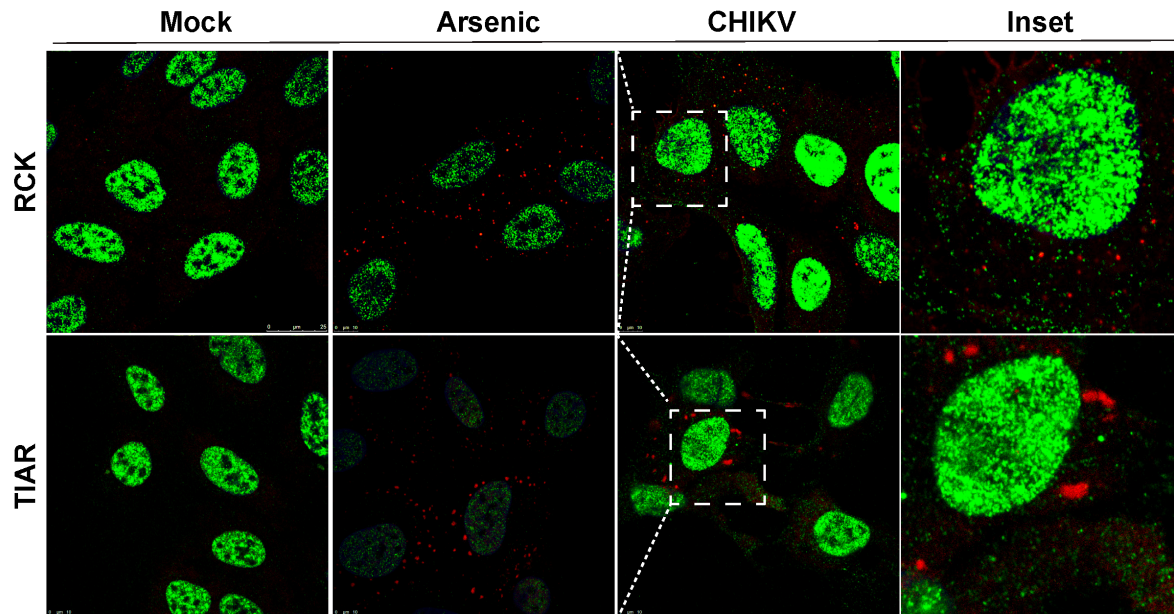


Figure S4. DDX39A does not colocalize with RNA processing bodies, Related to Figure 3. UO2S cells were infected with CHIKV- Ross (MOI5, 30h) or treated with arsenic for 30 minutes. Cells were then fixed, stained (anti-DDX39A in green and anti-RCK in red or TIAR in red, and nuclei, Hoechst 33342 in blue), and imaged with confocal microscopy, n=3. Scale bars shown.

Figure S5

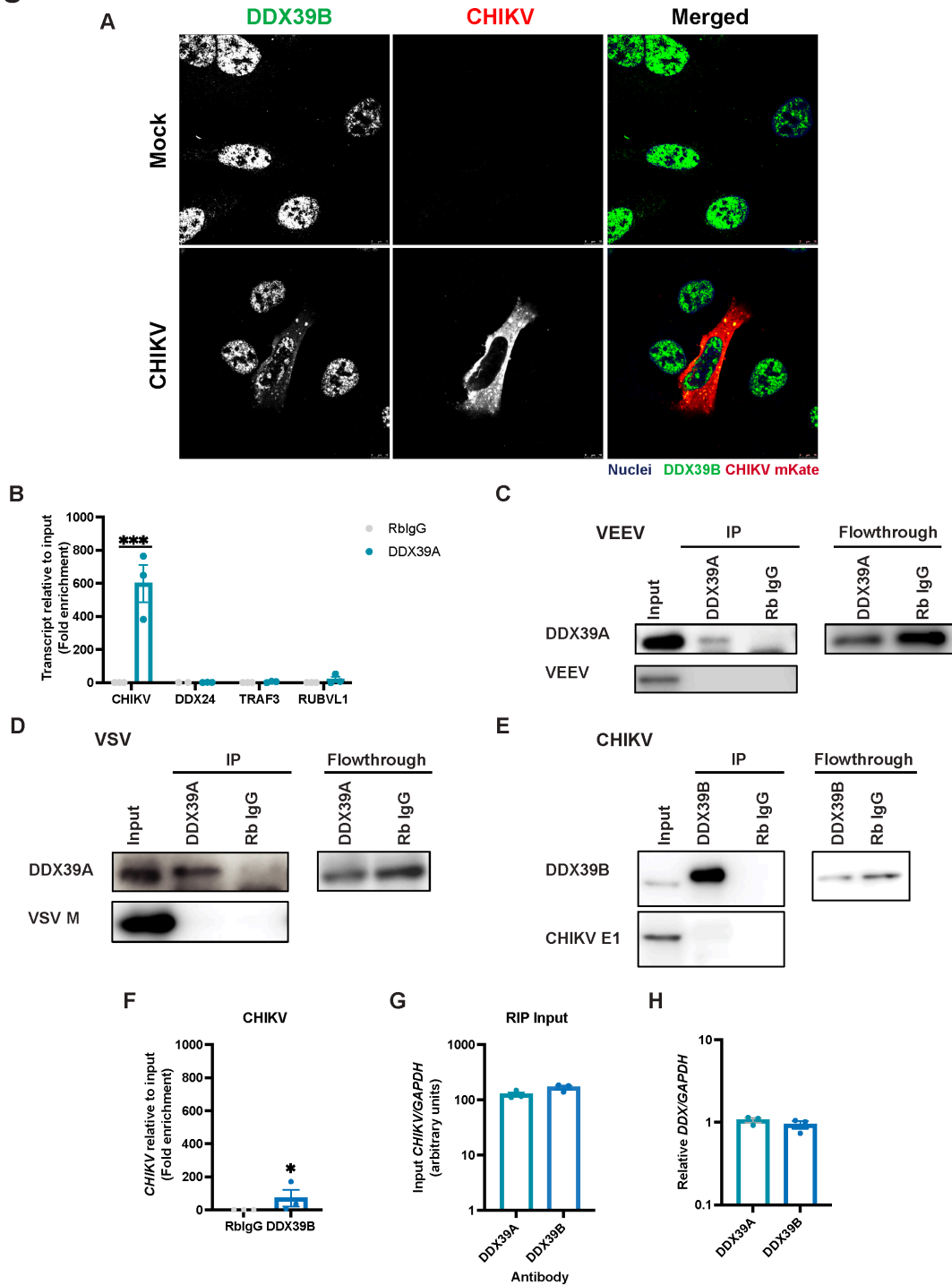


Figure S5. Endogenous DDX39A or DDX39B is immunoprecipitated to assess RNA binding by RIP-qPCR, Related to Figure 5.

(A) CHIKV-infected cells were stained with DDX39B (green) and Hoechst (nuclei, blue) at 20hpi. Representative images shown, n=3. Magnification 63x; Scale bar 10 μ m (B) CHIKV-infected U2OS cells were cross-linked at 20 hpi. Host genes or viral transcript associated with DDX39A or

with the rabbit IgG control were analyzed by qPCR. Enrichment was assessed relative to input. Data are shown fold change relative to the rabbit IgG control. (C) Endogenous DDX39A was immunoprecipitated for RIP-qPCR experiments upon infection with (C) VEEV and (D) VSV, representative immunoblots are shown. (E-F) Endogenous DDX39B was immunoprecipitated as shown by (E) immunoblot and (F) viral transcripts associated with DDX39B or the rabbit IgG control were analyzed by qPCR. (G) In RIP experiments done independently, CHIKV infection levels in inputs were assessed by qPCR. (H) Relative levels of DDX39A and DDX39B in U2OS were assessed by standard curve qPCR. Dots represent individual experiments, all experiments n=3. Statistical analyses were performed using one-way ANOVA with Bonferroni corrections (B), Student's (unpaired, two-tailed) *t*-test (F-H) **p*<0.05, ***p*<0.01, ****p*<0.001, *****p*<0.0001; error bars represent S.E.M.

Figure S6

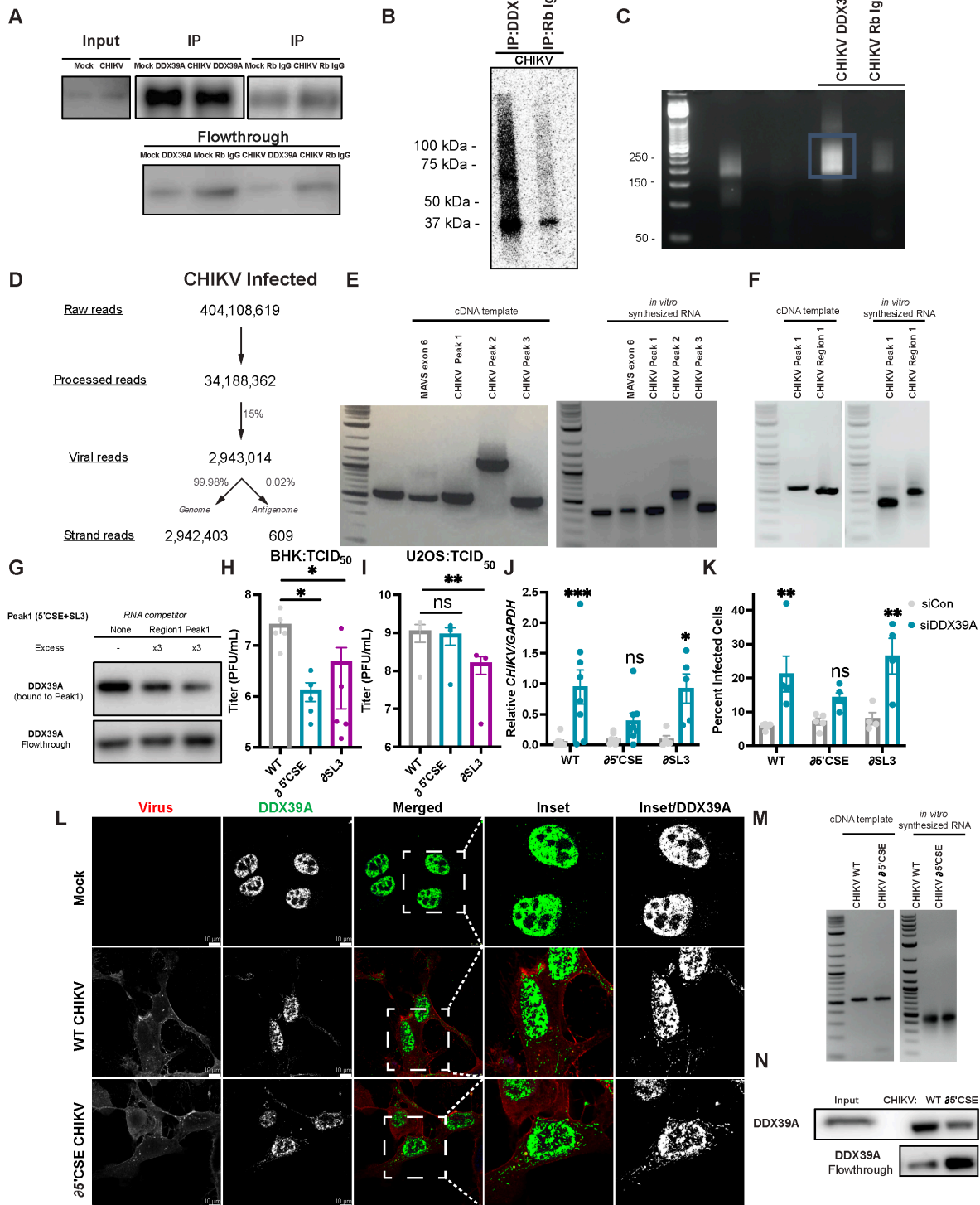


Figure S6. Mapping DDX39A-CHIKV RNA interactions using CLIP-seq and RNA affinity experiments, Related to Figure 5.

(A) Mock uninfected or CHIKV-infected cells were UV-crosslinked and immunoprecipitated with DDX39A or Rb IgG. Representative image of immunoblot. (B) After immunoprecipitation with

DDX39A or Rb IgG, samples were radiolabeled with ^{32}P , and ran on an SDS-PAGE gel for size selection. Representative image is shown after scanning with a Typhoon imager. (C) A 5' RNA adapter with a degenerate barcode was ligated to the extracted RNA and samples were reversed transcribed and amplified by PCR using primers with specific indexes to allow for demultiplexing of samples following sequencing. Representative image of PCR fragments shown. (D) Total raw reads from CHIKV-infected cells were trimmed, collapsed and biological replicates merged and mapped to a composite genome composed of the full human genome (hg38) and of the CHIKV genomic sequence (Ross strain; GenBank accession no. AF490259.3). Unique read counts were retrieved for each strand using Samtools. (E) The indicated fragments were PCR-amplified to create templates for *in vitro* RNA synthesis and RNA affinity. (F-G) CHIKV Peak 1 and Region 1 fragments were synthesized for RNA affinity competition between the biotinylated Peak 1-bound to streptavidin beads and excess unbiotinylated Peak-1 or Region-1 fragments in the presence of cell lysate. (G) Levels of DDX39A bound to the biotinylated Peak-1 relative to the unbiotinylated competing RNAs are compared by immunoblot. (H-I) WT, $\partial 5'$ CSE, or the ∂ SL3 were serially diluted and added to (H) BHK and (I) U2OS cells for 24h, and titer levels were assessed by TCID₅₀. (J-K) Control and DDX39A-depleted U2OS cells were infected with WT, $\partial 5'$ CSE or the ∂ SL3 strains of CHIKV for 24h, and viral levels were assessed by (J) qPCR and by (K) automated microscopy. (L) Mock uninfected or U2OS cells infected with WT and $\partial 5'$ CSE CHIKV (MOI 0.5, 20h) were fixed, stained (anti-DDX39A in green, anti-CHIKV in red, and nuclei, Hoechst 33342 in blue), and imaged with confocal microscopy, n=2. (M) Templates were created from purified WT and $\partial 5'$ CSE viruses for *in vitro* synthesis and then biotinylated. (N) WT and $\partial 5'$ CSE biotinylated RNAs were bound to streptavidin beads, incubated with lysate at 4°C, washed and the remaining protein on beads was assessed by immunoblot. Dots represent individual experiments, n=4-7 for all experiments. *GAPDH* was used as a loading control gene for all qPCR experiments. Statistical analyses were performed using one-way ANOVA with multiple comparisons (H, I), and two-way ANOVA with multiple comparisons (J, K). *p<0.05, **p<0.01, ***p<0.001, ****p<0.0001; error bars represent S.E.M.

Figure S7



Rank	Motif	P-value	log P-value	% of Targets	% of Background
1		1e-13	-3.175e+01	21.40%	11.99%
2		1e-13	-3.153e+01	21.89%	12.40%

Figure S7. DDX39A binding motifs for host genes, Related to Figure 5.

Frequency plot of two motifs identified by HOMER from DDX39A peaks in host transcripts. The “% of Targets” column indicates the % of DDX39A peaks containing the motif while the “% of Background” indicates the frequency of the motif in the background data.

Figure S8

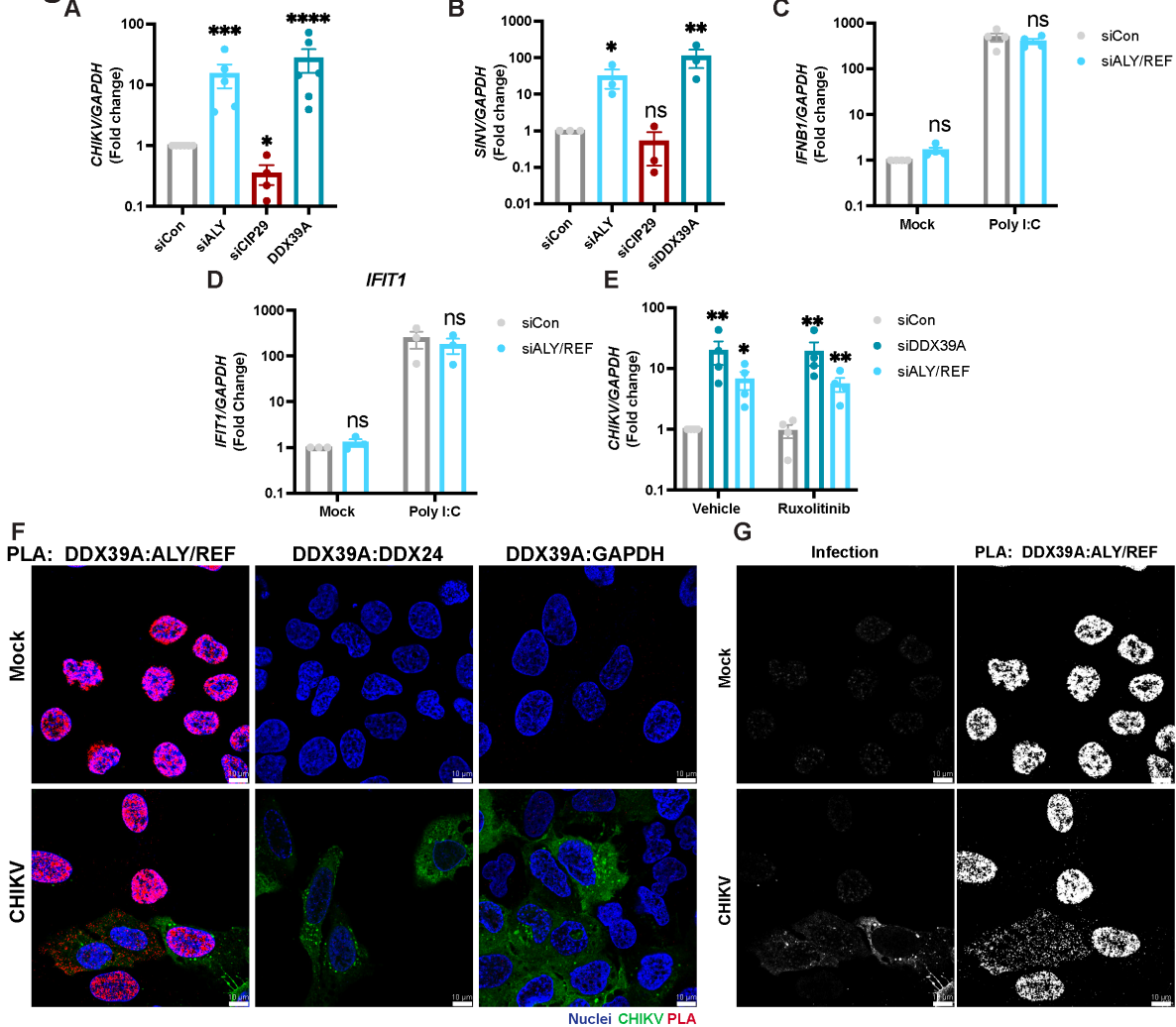


Figure S8 ALY-REF is antiviral against alphaviruses and associates with DDX39A in CHIKV-infected cells, related to Figure 5.

(A-B) Control and siRNA ALY/REF, CIP29, and DDX39A-depleted cells were infected with (A) CHIKV (MOI 0.5, 24h) and (B) SINV (MOI 0.1, 24h) and viral RNA was assessed by qPCR. (C-D) U2OS cells depleted of control and ALY/REF were transfected with either vehicle or poly (I:C) for 6-8h. Levels of (C) *IFNB1* and (D) *IFIT1* were assessed by qPCR. (E) U2OS cells depleted of control, ALY/REF, and DDX39A were pretreated with vehicle or Ruxolitinib, infected with CHIKV, and viral levels were quantified by qPCR. (F) Mock and CHIKV-infected U2OS cells were reacted with mouse and rabbit antibody pairs for DDX39A-ALY/REF, DDX39A-DDX24, and DDX39A-GAPDH and subjected to PLA by incubating with species specific PLA oligo probe tagged secondary antibodies, incubated with ligase and then amplification solution and fluorescently labeled oligonucleotides (red). Immunofluorescence with anti-CHIKV in red, and Hoechst (nuclei, blue) and cells were imaged with confocal microscopy, n=2. (G) Monochrome images of the left panel in F. Dots represent individual experiments, n=3-4 for all experiments. *GAPDH* was used as a loading control gene for all qPCR experiments. Statistical analyses were performed using one-way ANOVA with multiple comparisons (A, B), and two-way ANOVA with multiple comparisons (C, D, E). *p<0.05, **p<0.01, ***p<0.001, ****p<0.0001; error bars represent S.E.M.

Table S1. DDX screen, Related to Figure 1

Library	Gene Symbol	Avg_Zscore_TotalCells	Avg_Zscore_%Positive
Dharmacon	DDX1	0.476305476	0.007901562
Dharmacon	DDX10	0.140288395	0.481909761
Dharmacon	DDX11	0.275141847	-0.087999637
Dharmacon	DDX17	0.268602189	0.077356883
Dharmacon	DDX18	0.144467879	0.432583584
Dharmacon	DDX19A	0.431571327	0.140965862
Dharmacon	DDX19B	-0.290430039	-1.587683848
Dharmacon	DDX20	0.353816206	0.174766974
Dharmacon	DDX21	-0.26415485	-0.154159864
Dharmacon	DDX23	-0.617752506	0.551720292
Dharmacon	DDX24	-0.665711	-0.718320698
Dharmacon	DDX25	-0.2194996	0.316121046
Dharmacon	DDX27	0.283469586	0.402196388
Dharmacon	DDX28	0.445365569	-0.558207454
Dharmacon	DDX31	0.479725631	1.317873837
Dharmacon	DDX39	0.489242729	1.782054712
Dharmacon	DDX39B	-0.9894877	0.830854244
Dharmacon	DDX3X	-0.39232888	-1.157055802
Dharmacon	DDX3Y	0.330446311	0.852899203
Dharmacon	DDX4	0.383646361	0.157517763
Dharmacon	DDX41	0.064399568	0.030574769
Dharmacon	DDX42	-0.037926794	0.953311183
Dharmacon	DDX43	0.667432892	1.928539232
Dharmacon	DDX46	0.35444086	-0.218721897
Dharmacon	DDX47	-0.081385288	0.02628907
Dharmacon	DDX49	0.109261701	-0.147898261
Dharmacon	DDX5	0.0949275	-0.203557624
Dharmacon	DDX50	-0.344416672	2.866773293
Dharmacon	DDX51	0.42182489	-0.671295785
Dharmacon	DDX52	0.433935195	-0.294546657
Dharmacon	DDX53	0.290788719	-0.131220705
Dharmacon	DDX54	-0.134709836	-0.569582148
Dharmacon	DDX55	0.540234637	-0.353612599
Dharmacon	DDX56	-0.174245021	0.074929715
Dharmacon	DDX58	0.436485602	0.343085721

Dharmacon	DDX59	0.319156887	-0.889350625
Dharmacon	DDX6	-0.565601073	-0.844918108
Dharmacon	DDX60	0.337906675	0.536209938
Dharmacon	DDX60L	0.39005483	0.59445078
Dharmacon	EIF4A1	-1.849566092	-1.100473697
Dharmacon	EIF4A2	0.313807285	0.232675397
Dharmacon	EIF4A3	-6.053321537	-1.942119227

Table S3. CHIKV genome annotations, Related to Figure 5

Genome	Start	End	Viral RNA/protein
AF490259.3	76	7497	nonstructural polyprotein
AF490259.3	7566	11312	structural polyprotein
AF490259.3	1	75	UTR
AF490259.3	76	1680	nsP1
AF490259.3	1681	4074	nsP2
AF490259.3	4075	5664	nsP3
AF490259.3	5665	7497	nsP4
AF490259.3	7566	8348	C
AF490259.3	8349	8540	E3
AF490259.3	8541	9809	E2
AF490259.3	9810	9992	6K
AF490259.3	9993	11309	E1
AF490259.3	11313	11812	UTR
AF490259.3	1	11812	genome
AF490259.3	1	11812	antigenome
AF490259.3	7498	11812	subgenome

Genome name	Start	End	Secondary RNA structure
AF490259.3	70	156	SLE
AF490259.3	160	217	5'CSE
AF490259.3	2501	3079	Packaging signal
AF490259.3	5683	5754	Opal read-through stem
AF490259.3	9943	10033	Terminal frameshift
based on structures from Madden and colleagues ⁵			

Table S4. Recombinant virus sequences, Related to Figure 5

Virus strain	Mutant Name	Sequence range	Number mutations	Sequence
CHIKV 181/25	WT	67-220	0	ATAACCCATCATGGATTCTGTGTACGT GGACATAGACGCTGACAGCGCCTTTTT GAAGGCCCTGCAACGTGCGTACCCCA TGTTTGAGGTGGAACCTAGGCAGGTCA CATCGAATGACCATGCTAATGCTAGAG CGTTCTCGCATCTAGCCATA
CHIKV 181/25	∂5'CSE	67-220	10	ATAACCCATCATGGATTCTGTGTACGT GGACATAGACGCTGACAGCGCCTTTTT GAAGGCCCTGCAACGTGCGTACCCCA TGTTTGAGGTGGAACCTAGGCAGGTCA CATCTAACGACCATGCGAACGCCAGAG CGTTTACCCACCTAGCTATA
CHIKV 181/25	∂SL3	67-220	11	ATAACCCATCATGGATTCTGTGTATGT GGACATTGATGCTGACAGCGCGTTCCT CAAGGCGCTTCAACGTGCCTATCCCAT GTTTGAGGTGGAACCTAGGCAGGTCA CATCGAATGACCATGCTAATGCTAGAG CGTTCTCGCATCTAGCCATA

Table S5. Oligonucleotides, Related to STAR Methods (Oligonucleotides section)

Oligonucleotides			
siRNA name	Sense	Antisense	Source
DDX39A-1	CAGGACCGGUUUGAAG UUA	UAACUCAAACCGGU CCUG	Sigma
DDX39A-2	GAGUCAACAUCGUCUU UAA	UAAAAGACGAUGUUG ACUC	Sigma
DDX39B-1	AGUUCAUGCAAGAUC AAU	AUUGGAUCUUGCAUG AACU	Sigma
DDX39B-2	CAGUACUACGUGAAAC UGA	UCAGUUUCACGUAGU ACUG	Sigma
DDX39B-3	AGCUACUAGUGGAGCA GAA	UUCUGCUCCACUAGU AGCU	Sigma
ALY/REF-1	CAUUCAGCUUGUCACG UCA	UGACGUGACAAGCUG AAUG	Sigma
ALY/REF-2	GGAACUCUUUGCUGAA UUU	AAAUUCAGCAAAGAGU UCC	Sigma
CIP29-1	UGGUGAAAUUACAUC UGA	UCAGAUGUAAUUUUC ACCA	Sigma
CIP29-2	GCAAGAUCUUAUCCACA GA	UCUGUGGAUAAGAUC UUGC	Sigma
siFIT-1	GAGAAAAGCUAGACAAA AUTT	AUUUUGUCUAGCUUU UCUCTG	Sigma
siFIT-2	GGCUGUCCGCUUAAAU CCATT	UGGAUUUAAGCGGAC AGCCTG	Sigma

siCon			Lifetechnologies #AM4613
siDeath			Qiagen#1027299
qPCR Primer name			
	Forward	Reverse	Source
CHIKV nsp2	GGCAGTGGTCCCAGATA ATCAAG	ACTGTCTAGATCCACC CCATACATG	IDT
DDX39A	GAGCGAGTCAACATCGT CTTTA	AAGTGATGGCTAGGC CTTTG	IDT
IFIT1	CAACCAAGCAAATGTGA GGA	AGGGGAAGCAAAGAA AATGG	IDT
IFIT2	CACTGCAACCATGAGTG AGAA	AGTAGGTTGCACATTG TGGCT	IDT
IFIT3	AAAAGCCCAACAACCCA GAAT	CGTATTGGTTATCAGG ACTCAGC	IDT
IFIT5	GGGCTGGGGTCTCTCC TTTA	AATTTCACTCATGATG GCAGCG	IDT
IKBa	CTCCGAGACTTTCGAGG AAATAC	CCATTGTAGTTGGTAG CCTTCA	IDT
IRF7	GTGTGTCTTCCCTGGAT AGC	GGAGTTCTCATTAGAC TGGGTTT	IDT
IFNB1	CAACTTGCTTGGATTCC TACAAAG	TATTC AAGCCTCCCAT TCAATTG	IDT
ALY/REF	GTGGAGACAGGTGGGA AAC	CCTTCTTCAGCGTTCC AAATTC	IDT
CIP29	GAAGTGAACACAGAG GATAC	CTGGAGAACAGAAAGT ATCAGGAA	IDT
GAPDH	ACCAAATCCGTTGACTC CGACCTT	TCGACAGTCAGCCGC ATCTTCTTT	IDT
SINV nsp1	GCTGAAACACCATCGCT CTGCTTT	TGGTGTGGAAGCCAAT CCAGTACA	IDT
RVFV	CAAGCAGTGGACCGCA ATGAGA	GGGCTTGTTGCCACG AGTTAGA	IDT
229E	TGGCGGGTGGGATAATA TGT	GAGGGCATAGCTCTAT CACACTTAGG	IDT
OC43	CTATCTGGGAACAGGAC CGC	TTGGGTCCCGATCGAC AATG	IDT
ONNV	CGGCACTCTTCGCAAAA ACA	TCCTCGGTGTGCTTTG TACC	IDT
VSV	CGGAGGATTGACTAATG C	ACCATCCGAGCCATT C	IDT
VEEV	GTGTGACCAAATGACTG	ACCGTTGACGACTATA C	IDT
DDX24	TTGACCCTGCATGCCTG TAT	AGGAATATCCAGACCC CGAG	IDT
TRAF3	CTCACAAGTGCAGCGTC CAG	GCTCCACTCCTTCAGC AGGTT	IDT

CHIKV (-) antigenome cDNA	GGCAGTATCGTGAATTC GATGCCGCTGTACCGTC CCCATTCC		Meertens, et al. ⁶
CHIKV (-) antigenome qPCR	GGCAGTATCGTGAATTC GATGC	ACTGCTGAGTCCAAAG TGGG	Meertens, et al. ⁶
gBlock CHIKV Anti- Genome Amplicon Standard:	GGCAGTATCGTGAATTC GATGCCGCTGTACCGTC CCCATTCCAGAACACAC TACAGAAATGACTGGCA GCAGCCACGAAAAGAAA CTGCAACGTCACACAGA TGAGGGAATTCACCACT TTGGACTIONCAGCAGT		Meertens, et al. ⁶

Oligos for RNA synthesis

	Forward	Reverse	
CHIKV- Peak1	ATGGCTGCGTGAGACAC AC	ACGTCTGCTCTCTGTC TACAT	This paper
CHIKV- Peak2	CGATGGTGTACAACGAA AGAGA	CCAACTCTTAGCCCA ACAAAC	This paper
CHIKV- Peak3	ATGGAGTTCATCCCAAC CCA	AGGTCGTACTIONTAGATG ACCGC	This paper
CHIKV- Region1	CTTCATCGGCGACGACA ACA	TAGGTAGCTGTAGTGC GTACC	This paper
MAVS	GGGCTGTGTCTCCATC T	TTCTGCTGCTCCCGT CA	This paper
DDX24	TCCCACGTACCTCGGAG ATTTATG	GCA GAC TCG CTC TTA CTT GGG	This paper

Oligos used in CLIP-Seq

oligo name	IDENTIFIER/SEQUENCE	SOURCE	REF.
RL5D	/5InvddT/rArGrGrGrArGrGr ArCrGrArUrGrCrGrGr(N1:2 5252525)r(N1)r(N1)r(N1)r G	IDT	Vourekas and Mourelatos ⁷
RL3(+P)	/5Phos/rGrUrGrUrCrArGrU rCrArCrUrUrCrCrArGrCrGr G/3InvdT/	IDT	Vourekas and Mourelatos ⁷
RL3(-P)	rGrUrGrUrCrArGrUrCrArCr UrUrCrCrArGrCrGrG/3Invd T/	IDT	Vourekas and Mourelatos ⁷
P3-*C*A*C	CCGCTGGAAGTGACTIONGA *C*A*C	IDT	Vourekas and Mourelatos ⁷
DP5	AGGGAGGACGATGCGG	IDT	Vourekas and Mourelatos ⁷
MSFP3	CAAGCAGAAGACGGCAT ACGAGATCCGCTGGAA GTGACTIONGACAC	IDT	Vourekas and Mourelatos ⁷

Index primers	AATGATACGGCGACCAC CGAGATCTACACTCTTT CCCTACACGACGCTCTT CCGATCT[index]AGGGA GGACGATGCGG	IDT	Vourekas and Mourelatos ⁷
	(index sequences: CTAG,GATC,CGTA,GCAT ,GTGC,ACCG,CATG,TGC A,TCAC,AGTG,TACG,CC GA)		

Supplemental References

1. Guzmán-Terán, C., Calderón-Rangel, A., Rodríguez-Morales, A., and Mattar, S. (2020). Venezuelan equine encephalitis virus: The problem is not over for tropical America. *Annals of clinical microbiology and antimicrobials* *19*, 1-8.
2. Mehta, R., Gerardin, P., de Brito, C.A.A., Soares, C.N., Ferreira, M.L.B., and Solomon, T. (2018). The neurological complications of chikungunya virus: A systematic review. *Reviews in medical virology* *28*, e1978.
3. Baxter, V.K., and Heise, M.T. (2020). Immunopathogenesis of alphaviruses. *Advances in virus research* *107*, 315-382.
4. Rezza, G., Chen, R., and Weaver, S.C. (2017). O'nyong-nyong fever: a neglected mosquito-borne viral disease. *Pathog Glob Health* *111*, 271-275. 10.1080/20477724.2017.1355431.
5. Madden, E.A., Plante, K.S., Morrison, C.R., Kutchko, K.M., Sanders, W., Long, K.M., Taft-Benz, S., Cisneros, M.C.C., White, A.M., Sarkar, S., et al. (2020). Using SHAPE-MaP To Model RNA Secondary Structure and Identify 3'UTR Variation in Chikungunya Virus. *Journal of Virology* *94*, e00701-00720. 10.1128/JVI.00701-20.
6. Meertens, L., Hafirassou, M.L., Couderc, T., Bonnet-Madin, L., Kril, V., Kümmerer, B.M., Labeau, A., Brugier, A., Simon-Lorier, E., and Burlaud-Gaillard, J. (2019). FHL1 is a major host factor for chikungunya virus infection. *Nature* *574*, 259-263.
7. Vourekas, A., and Mourelatos, Z. (2014). HITS-CLIP (CLIP-Seq) for mouse Piwi proteins. In *PIWI-Interacting RNAs*, (Springer), pp. 73-95.